Steady State Simulation of the Operation of an Evaporative Cooled Water-Ammonia Absorption Scale Ice Maker with Experimental Basis

Rodolfo Jesús R. Silverio
rodolfo@fsjb.edu.br
Faculdade de Aracriz - UNIARACRUZ
Aracruz, ES. Brazil

José Ricardo Figueiredo
jrfigue@fem.unicamp.br
State University of Campinas – UNICAMP
Faculty of Mechanical Engineering
Cx. Postal 6122
130883-970 Campinas, SP. Brazil

A steady-state model is presented of the operation of a water-ammonia absorption system for production of scale ice. The model involves relations of thermodynamics, heat transfer, and fluid mechanics, and uses simplifying assumptions for the internal mass transfer processes, leading to a non-linear system with more than 100 unknowns and equations, that are reduced to a dimension-10 Newton-Raphson problem by means of the Substitution-Newton-Raphson approach. The model was validated against experimental data with good agreement.
***Keywords**: Absorption refrigeration, ammonia water, icemaker, computational simulation, Newton-Raphson method*

Introduction

The increasing cost of electricity and the environmental hazard of CFCs have made the absorption water-ammonia heat-powered cooling systems attractive for both residential and industrial applications. The development of this technology demands reliable and effective system simulations; several computer models have been developed, and have proved to be valuable tools for thermal design optimization (Vliet *et al.*, 1982; Molt, 1984; McLinden and Klein, 1985; Grossman *et al*., 1985,1987,1990). However, there are few models taking into account the heat and mass transfer characteristics in absorption systems for scale ice making and for evaporative exchangers.

This work presents a mathematical model for such a system, taking into account thermodynamic, heat transfer and fluid mechanics phenomena, and adopting simplifying assumptions for the internal mass transfer processes. It involves both constructive and external parameters in order to simulate numerically the steady-state performance of a scale icemaker based on an absorption refrigeration system. The model was successfully validated against experimental data.

The experimental system is a water-ammonia absorption refrigeration machine with nominal refrigeration capacity for scale ice production of 23,25 kW, located at the Hospital das Clínicas of the State University of Campinas (UNICAMP), Brazil. The machine is driven by a small part of the vapor produced for consumption in the hospital. Ice is produced directly on the evaporator surface, and the machine heat rejection is done via evaporative cooled absorber, condenser and weak solution cooler. Heat and mass transfer coefficients for the simulation were estimated from a set of processed experimental data.

Figure 1 sketches the refrigeration system. Evaporator E, expansion valve EV and condenser C operate as in a mechanical compression refrigeration system, with the remaining components playing the role of a compressor.

The vapor leaving the evaporator is absorbed by the weak solution in absorber A forming the strong solution, which is driven by solution pump SP to the generator. This is composed of desorber D, where ammonia vapor is liberated with a water content still too high for the evaporator, and the components that remove most of the water: distillation column DC and reflux condenser RC. The part of the vapor which is condensed in the RC returns as reflux (R) to DC where it exchanges heat and mass with the ascending vapor. After the reflux condenser, the ammonia vapor is admitted to the condenser C.

The ammonia sub-cooler ASC increases the amount of liquid to be evaporated, and the solution heat exchanger SHx pre-heats the strong solution while pre-cooling the weak solution that leaves the desorber, thus reducing the amount of external heat needed, and also decreasing the required size for both the desorber and the absorber. In the weak solution cooler WSC this solution is cooled before entering the absorber.

In order to reduce initial costs, the evaporative cooled components, namely condenser, absorber and weak solution cooler, are located in a single evaporative tower.

Reservoir R_1, [R_1 ,] for the nearly pure ammonia leaving the condenser, ensures the constant pressure in the evaporator, and reservoir R_2, for the strong solution leaving the absorber, guarantees that only liquid enters into the solution pump.

Because of the ice formation itself, the system operation is cyclically transient. Ice forms directly on the evaporator walls, requiring a defrost process lasting for about 1 to 1.5 minutes , much shorter than the ice-making period of 10 to 20 minutes. For defrosting, the liquid within the evaporator is blown down to the absorber while the evaporator is filled with vapor taken from the condenser, warming the evaporator walls, and causing the ice to fall down.

At the beginning of the ice-making period, ice formation is quick, and gets slower as the ice layer gathers on the evaporator walls, because of the increased heat transfer resistance; both the evaporation temperature and the overall performance diminish. Thus, a transient model of the operation is important for determining the optimum ice-making period, as will be shown in another paper.

The present steady state modeling is a necessary first step towards such a transient model, but it is also very important by itself, because it reflects the mean operating conditions, providing useful information on the overall system performance.

Furthermore, it had been observed that only parts of the system are affected by the transient operation basically the evaporator, as explained above, and the absorber, which warms significantly above its mean temperature after receiving the liquid ammonia at the beginning of the defrost. The other components, in contrast, are only slightly affected. The vapor mass taken from the condenser in the defrost period is small. The liquid mass required to fill the evaporator after the defrost is much more significant, but it is taken from the reservoir under the condenser which is refilled gradually, so that the high-pressure side of the system is nearly unaffected by the defrost.

Paper accepted June, 2006. Technical Editor: Atila P. Silva Freire.

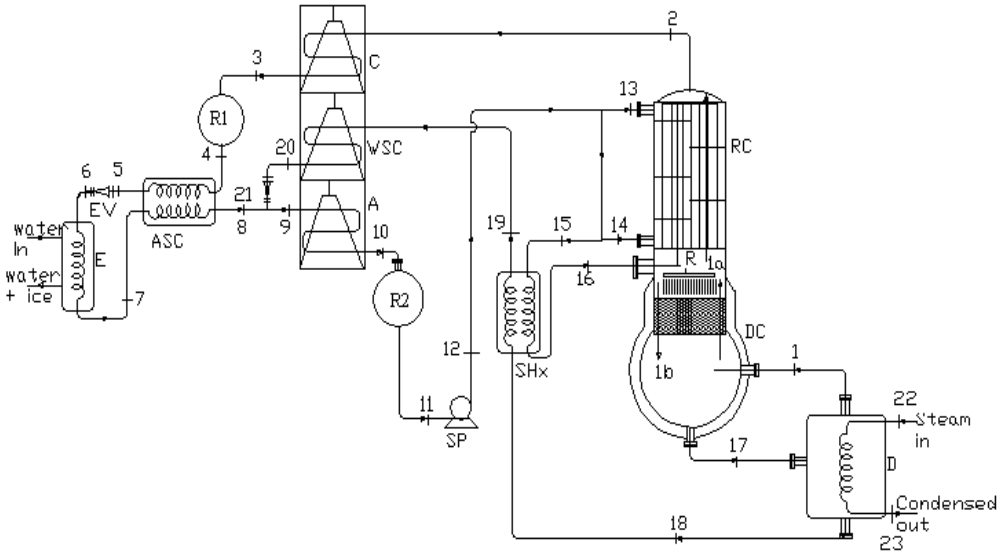

Figure 1. Basic representation of the system.

Nomenclature

Latin Symbols

A = *heat transfer surface* [m^2]
COP = *coefficient of performance*
$C_F$thermal = *capacity of the fluid* [*J/ºC*]
C_F = *thermal capacity of the fluid* [W/ºC]
D = *diameter of tubes and pipes* [*m*]
DEV = *deviation from equilibrium*
EV = *expansion valve*
f = *real function*
F = *correction coefficient for mean temperature difference*
g = *real function*
h = *specific enthalpy* [*J/kg*]
H = *heat of liquid-solid phase change* [*J/kg*]
K= *coefficient for localized head loss*
K_M = *mass transfer coefficient in evaporative tower*
L = *tube and pipe lengths*
$\dot{m}$ = *mass flow rate* [*kg/s*]
N = *number of physically relevant variables*
n = *number of effective variables in the SNR method* (*n*<*N*)
NTU = *number of transfer units*
P = *pressure* [*Pa*]
Q = *heat rate* [*W*]
Re = *Reynolds number*
T = *temperature* [*K, unless otherwise stated*]
U = *global heat transfer coefficient* [$W/(m^2K)$],
U = *dryness degree of the vapor-liquid mixture*
v = *specific volume of water-ammonia solution*
X = *mass concentration of ammonia in the liquid solution*
Y = *mass concentration of ammonia in the vapor solution*
Z = *total mass concentration of ammonia,*

Greek Symbols

Δ = *difference or increment in variable*
ε = *relative roughness of pipes [m]*
ς = *relative roughness of tubes*
$-\eta$ = *efficiency*
ρ = *fluid density* [kg/m^3]
ϕ = *coefficient of viscosity correction*
λ = *friction factor*

Subscripts

1,2... = *index of ordering*
A = *absorber*
air = *relative to cooling air*
ASC = *ammonia sub-cooler*
C = *condenser*
D = *desorber*
E = *evaporator*
f = *fluid*
H = *hydraulic*
p = *pipe*
RC = *reflux condenser*
sat = *saturation*
SHx = *solution heat exchanger*
SP = *solution pump*
st = *steam*
t = *tube*
w = *wall*
wb =*welt bulb*
WSC = *weak solution cooler*

Superscripts

0 = *zero centigrade degree on water-ice interface*
A = *available in NTU*
i = *interface*
In= relative to air inlet air flow
L = *liquid*
Out = relative to air outlet air flow
R = *required in NTU*
(0) = *relative to water*
(1) = *relative to ammonia*
SS = *strong solution*
Teva = *temperature of evaporation*
V = *vapor*
WS = *weak solution*

Steady State Model

This steady-state model simulated the mean operating condition of the system. Each component was treated as an independent

control volume with its own inputs and outputs. The model equations are presented below for each component. These equations represent conservation of the total mass, conservation of the mass of ammonia, conservation of the energy (assuming negligible kinetic and potential energy variations between the inlet and outlet fluxes), the phenomenological equations of heat transfer and of pressure drops, and the thermodynamic state relations for the mixture. A more detailed presentation can be found in Silverio (1999).

Desorber

In the desorber, heat is supplied by means of steam to boil off ammonia from the water-ammonia mixture. Point 1 in the desorber was considered in equilibrium with the liquid leaving the generator at point 18. The rate of condensation of the vapor feeding the desorber could be easily measured by collecting the condensed liquid in a calibrated vessel.

$$\dot{m}_{17} - \dot{m}_1 - \dot{m}_{18} = 0 \qquad (01)$$

$$\dot{m}_{17}X_{17} - \dot{m}_1Y_1 - \dot{m}_{18}X_{18} = 0 \qquad (02)$$

$$\dot{m}_{17}h_{17} - \dot{m}_1h_1 - \dot{m}_{18}h_{18} + \dot{Q}_D = 0 \qquad (03)$$

$$\dot{m}_{22}(h_{22} - h_{23}) - \dot{Q}_D = 0 \qquad (04)$$

$$(UA)_D \frac{(T_{18} - T_{17})}{\ln\dfrac{(T_{17} - T_{22})}{(T_{18} - T_{22})}} - \dot{Q}_D = 0 \qquad (05)$$

$$T_{18} = T_{sat}(P_{18}, X_{18}) \qquad (06)$$

$$T_1 = T_{18} \qquad (07)$$

$$P_1 = P_{18} \qquad 08)$$

$$Y_1 = Y_{sat}(P_1, T_1) \qquad (09)$$

$$h_{22} = h''(P_{steam}) \qquad (10)$$

$$h_{23} = h'(P_{steam}) \qquad (11)$$

$$h_1 = h_{vap}(P_1, T_1, Y_1) \qquad (12)$$

$$h_{17} = h_{liq}(P_{17}, T_{17}, X_{17}) \qquad (13)$$

$$h_{18} = h_{vap}(P_{18}, T_{18}, X_{18}) \qquad (14)$$

Distillation Column

The column is adiabatic, and it is assumed that there is no resistance to the mass transfer between liquid and vapor in countercurrent. The possibility of strong solution vaporization in the solution heat exchanger is taken into account by introducing the dryness of the mixture into the balances.

$$\dot{m}_r + \dot{m}_1 + \dot{m}_{16}(1 - U_{16}) - \dot{m}_{17} - \dot{m}_{1a} = 0 \qquad (15)$$

$$\dot{m}_rX_r + \dot{m}_1Y_1 + \dot{m}_{16}(1 - U_{16})X_{16} - \dot{m}_{17}X_{17} - \dot{m}_{1a}Y_{1a} = 0 \qquad (16)$$

$$\dot{m}_rh_r + \dot{m}_1h_1 + \dot{m}_{16}(1 - U_{16})h_{16}^L - \dot{m}_{17}h_{17} - \dot{m}_{1a}h_{1a} = 0 \qquad (17)$$

Reflux Condenser

In the reflux condenser, vapor leaving the distillation column is partially condensed by the cool strong solution from the absorber and the solution pump. While it is cooled and partially condensed, the vapor exchanges mass with the condensed liquid, called reflux, in the top of the condenser, increasing its concentration. The temperature of the vapor leaving the reflux condenser, $T_{2,}$ was regarded as constant because it is assumed that it can be controlled the bypass in 13.

$$\dot{m}_{1a} + \dot{m}_{16}U_{16} - \dot{m}_2 - \dot{m}_r = 0 \qquad (18)$$

$$\dot{m}_{1a}Y_{1a} + \dot{m}_{16}U_{16}Y_{16} - \dot{m}_2Y_2 - \dot{m}_rX_r = 0 \qquad (19)$$

$$\dot{m}_{1a}h_{1a} + \dot{m}_{16}U_{16}h_{16}^V - \dot{m}_2h_2 - \dot{m}_rh_r = \dot{Q}_{RC} \qquad (20)$$

$$\dot{m}_{13}(h_{13} - h_{14}) = \dot{Q}_{RC} \qquad (21)$$

$$(UA)_{RC} \frac{(T_2 - T_{13}) - (T_r - T_{14})}{\ln\dfrac{(T_2 - T_{13})}{(T_r - T_{14})}} - \dot{Q}_{RC} = 0 \qquad (22)$$

$$Y_2 = Y_{sat}(P_2, T_2) \qquad (23)$$

$$T_r = T_2 \qquad (24)$$

$$X_r = X_{sat}(P_2, T_r) \qquad (25)$$

$$P_2 = P_{1a} - \Delta P_{RC}^V \qquad (26)$$

$$P_{14} = P_{13} - \Delta P_{RC}^L \qquad (27)$$

$$h_2 = h_{vap}(P_2, T_2, Y_2) \qquad (28)$$

$$h_r = h_{liq}(P_2, T_r, X_r) \qquad (29)$$

Ammonia Sub-Cooler

In the ammonia sub-cooler, liquid ammonia from the condenser is in thermal contact with ammonia vapor leaving the evaporator. This heat exchanger has 4 liquid internal passes for the liquid, and requires a correction factor for the LMTD, which is calculated according to Kern (1950).

$$\dot{m}_4(h_4 - h_5) - \dot{Q}_{ASC} = 0 \qquad (30)$$

$$m_7(h_8 - h_7) - \dot{Q}_{ASC} = 0 \qquad (31)$$

$$(UA)_{ASC}F_{ASC} \frac{(T_5 - T_7) - (T_4 - T_8)}{\ln\dfrac{(T_5 - T_7)}{(T_4 - T_8)}} - \dot{Q}_{ASC} = 0 \qquad (32)$$

with

$$F_{ASC} = \frac{\sqrt{R^2+1}\ln\left(\dfrac{1-S}{1-RS}\right)}{(R-1)\ln\left(\dfrac{2-S(R+1-\sqrt{R^2+1})}{2-S(R+1+\sqrt{R^2+1})}\right)} \qquad (33)$$

$$R = \frac{T_4 - T_5}{T_8 - T_7} \cong \frac{Cp^{V}_{NH_3}}{Cp^{L}_{NH_3}} \quad (34)$$

$$S = \frac{T_8 - T_7}{T_4 - T_7} \quad (35)$$

$$T_8 = T(h_8, P_8, Y_8) \quad (36)$$

$$T_4 = T_3 \quad (37)$$

$$Y_8 = X_3 \quad (38)$$

$$P_5 = P_4 - \Delta P^{L}_{ASC} \quad (39)$$

$$P_8 = P_7 - \Delta P^{V}_{ASC} \quad (40)$$

$$h_5 = h_{liq}(P_5, T_5, X_5) \quad (41)$$

$$h_7 = h_{vap}(P_7, T_7, Y_7) \quad (42)$$

Expansion Valve

Expansion takes place in a throttling valve and is considered adiabatic.

$$h_6 = h_5 \quad (43)$$

$$Z_6 = X_5 \quad (44)$$

$$T_6 = T(h_6, P_6, Z_6) \quad (45)$$

Evaporator

Ice is produced directly on the evaporator walls. This ice layer is the main resistance to the heat transfer between the water and the evaporating ammonia.

$$\dot{m}_6(h_7 - h_6) - \dot{Q}_E = 0 \quad (46)$$

$$\dot{m}_{ice}(Cp_{ice}\Delta T\big|_{T_{ice}}^{0} + H^{0}_{ice} + Cp_w \Delta T\big|_{0}^{T_{env}}) - \dot{Q}_E = 0 \quad (47)$$

$$(UA)_E \frac{(T_7 - T_6)}{\ln \frac{(T_6 - 0)}{(T_7 - 0)}} - \dot{Q}_E = 0 \quad (48)$$

$$Z_7 = Z_6 \quad (49)$$

$$P_7 = P_6 - \Delta P_E \quad (50)$$

Solution Heat Exchanger (Strong Solution Heater)

This is a horizontal countercurrent heat exchanger formed by three tubes in a shell; the hot weak solution flows inside the tubes, and the cold strong solution outside them.

$$\dot{m}_{18}(h_{18} - h_{19}) - \dot{Q}_{SHx} = 0 \quad (51)$$

$$\dot{m}_{15}(h_{16} - h_{15}) - \dot{Q}_{SHx} = 0 \quad (52)$$

$$(UA)_{SHx} \frac{(T_{19} - T_{15}) - (T_{18} - T_{16})}{\ln \frac{(T_{19} - T_{15})}{(T_{18} - T_{16})}} - \dot{Q}_{SHx} = 0 \quad (53)$$

$$P_{19} = P_{18} - \Delta P^{WS}_{SHx} \quad (54)$$

$$P_{16} = P_{15} - \Delta P^{SS}_{SHx} \quad (55)$$

$$h_{16} = h(P_{16}, T_{16}, X_{16}) \quad (56)$$

$$h_{19} = h(P_{19}, T_{19}, X_{19}) \quad (57)$$

Solution Pump

$$h_{12} - h_{11} - \frac{v_{11}(P_{12} - P_{11})}{\eta_P} = 0 \quad (58)$$

$$P_{11} = P_{10} - \Delta P_{Filters} \quad (59)$$

$$P_{12} = P_1 + \Delta P^{L}_{RC} + \Delta P^{SS}_{SHx} \quad (60)$$

$$v_{11} = h(P_{11}, T_{11}, X_{11}) \quad (61)$$

Evaporative Exchangers

The simulation of the evaporative heat exchangers (condenser, absorber and weak solution cooler) is based on Webb (1984), following Merkel, who identified the air enthalpy difference as the fundamental mechanism for the simultaneous heat and mass transfer in air-water vapor systems. There are more elaborated models for theses systems (Leindenfrost and Korenic, 1982) but in general the industry prefers the Webb approximate model , used in this work.

Condenser

$$\dot{m}_2(h_2 - h_3) + \dot{m}_{air\,C}(h^{Out}_{airC} - h^{In}_{air}) = 0 \quad (62)$$

$$\ln \frac{h^{i}_{airC} - h^{In}_{air}}{h^{i}_{airC} - h^{Out}_{airC}} = \frac{K_M}{U_C} \frac{h^{Out}_{airC} - h^{In}_{air}}{T_3 - T^{i}_{C}} \quad (63)$$

$$(NTU)^{R}_{C} - (NTU)^{A}_{C} = 0 \quad (64)$$

$$NTU^{R}_{C} = \frac{h^{i}_{airC} - h^{In}_{air}}{h^{i}_{airC} - h^{Out}_{airC}} \quad (65)$$

$$NTU^{A}_{C} = \frac{K_M A_C}{\dot{m}_{arC}} \quad (66)$$

$$T_3 = T_{sat}(P_3, X_3) \quad (67)$$

$$X_3 = Y_2 \quad (68)$$

$$P_3 = P_2 - \Delta P_C \quad (69)$$

Absorber

$$\dot{m}_9 - \dot{m}_8 - \dot{m}_{21} = 0 \quad (70)$$

$$\dot{m}_9 X_9 - \dot{m}_8 Y_8 - \dot{m}_{21} X_{21} = 0 \quad (71)$$

$$\dot{m}_9 h_9 - \dot{m}_8 h_8 - \dot{m}_{21} h_{21} = 0 \quad (72)$$

$$\dot{m}_9 (h_9 - h_{10}) + \dot{m}_{air\,A} (h_{airA}^{Out} - h_{air}^{In}) = 0 \quad (73)$$

$$\frac{T_9 - T_A^i}{T_{10} - T_A^i} = \frac{h_{airA}^i - h_{air}^{In}}{h_{airA}^i - h_{airA}^{Out}} \exp\left(\frac{U_A \dot{m}_{airA}}{C_{FA} K_M} \right) \quad (74)$$

$$C_{FA} = \dot{m}_9 Cp = \frac{Q_A}{(T_9 - T_{10})} \quad (75)$$

$$(NTU)_A^R - (NTU)_A^A = 0 \quad (76)$$

$$NTU_A^R = \frac{h_{airA}^i - h_{air}^{In}}{h_{airA}^i - h_{airA}^{Out}} \quad (77)$$

$$NTU_A^A = \frac{K_M A_A}{\dot{m}_{airA}} \quad (78)$$

$$T_{10} = T_{sat}(P_{10}, X_{10}) \quad (79)$$

$$P_{10} = P_9 - \Delta P_A \quad (80)$$

$$h_{10} = h_{liq}(P_{10}, T_{10}, X_{10}) \quad (81)$$

Weak Solution Cooler

$$\dot{m}_{20} (h_{20} - h_{21}) + \dot{m}_{air\,WSC} (h_{airWSC}^{Out} - h_{air}^{in}) = 0 \quad (82)$$

$$\frac{T_{20} - T_{WSC}^i}{T_{21} - T_{WSC}^i} = \frac{h_{airWSC}^i - h_{air}^{In}}{h_{airWSC}^i - h_{airWSC}^{Out}} \exp\left(\frac{U_{WSC} \dot{m}_{airWSC}}{C_{F\,WSC} K_M} \right) \quad (83)$$

$$C_{F\,WSC} = \dot{m}_{20} Cp = \frac{\dot{Q}_{WSC}}{(T_{20} - T_{21})} \quad (84)$$

$$(NTU)_{WSC}^R - (NTU)_{WSC}^A = 0 \quad (85)$$

$$NTU_{WSC}^R = \frac{h_{airWSC}^i - h_{air}^{In}}{h_{airWSC}^i - h_{airWSC}^{Out}} \quad (86)$$

$$NTU_{WSC}^A = \frac{K_M A_{WSC}}{\dot{m}_{airWSC}} \quad (87)$$

$$P_{21} = P_{20} - \Delta P_{WSC} \quad (88)$$

Other Equations

The thermodynamic state relations previously referred are reproduced according to the method of Schultz (1971) modified by Ziegler and Trepp (1984). The method is based on two fundamental equations for the Gibbs free energy in terms of temperature, pressure and concentration, one for the liquid phase and one for the vapor phase, in such a way that the values from both equations match at saturation conditions. The liquid solution is taken as a non-ideal mixture, and the vapor mixture is assumed to be an ideal solution of non-ideal gases.

Pressure losses in the above equations are determined for both the pipes and accessories along the flow circuit, and for each exchanger of the system. These pressure losses include the distributed friction losses (ΔP_{dist}) and the localized losses (ΔP_{loc}) in contractions, expansions, direction flow changes and nozzles at the inlet and outlet of the exchangers, computed as:

$$\Delta P_{dist} = \lambda \frac{L_p}{D_p} \frac{\rho V^2}{2} \text{ is the distributed loss in pipes do to friction} \quad (89)$$

$$\Delta P_{loc} = K \frac{\rho V^2}{2} \text{ is the localized loss} \quad (90)$$

The friction factor λ is determined by means of the equation due to Churchill (1977), multiplied by factor 8 to convert to a form suitable for Eq. (96) (89). For the pressure losses in the exchangers, calculations depend on the kind of exchanger, and on whether the flow is inside the tube or in the shell. The coefficients for pressure losses in components and in lines, computed according to Kern (1950), are reproduced in tTable 1. The evaporator and the generator are considered as large reservoirs with no pressure loss.

Table 1. Coefficients for pressure losses calculations in components and lines.

Component/Line	Flow area [m^2]	ε /D_H	$\Sigma(L/D_H)$	$\Sigma(K)$
Absorber	3,54e-03	0,0020	1050	10,50
Ammonia sub-cooler – liquid side	8,55e-04	0,0026	252	3,35
Ammonia sub-cooler – vapor side	1,25e-03	0,0018	86,5	1,4
Condenser	4,05e-03	0,0020	1050	10,50
Reflux Condenser - liquid side	3,32e-05	0,0077	92,30	1,40
Reflux Condenser - vapor side	6,08e-03	0,0036	47,25	1,33
SHx – weak solution side	1,27e-04	0,0040	4677	20,00
SHx – strong solution side	4,36e-05	0,0067	7973	20,00
Weak solution cooler	8,55e-04	0,0020	1050	10,50
Line 1	1,14e-03	0,0013	32,65	0,85
Line 2 – 6	1,27e-04	0,0039	1314,28	33,3
Line 7 – 8	5,07e-04	0,0020	472,52	25,4
Line 9	5,07e-04	0,0020	0,47	4,3
Line 10 – 11	5,07e-04	0,0029	111,88	38,7
Line 12 – 16	1,27e-0,4	0,0029	709,66	41,6
Line 17	1,14e-03	0,0013	25,85	0,49
Line 18 – 21	1,27e-04	0,0029	551,82	22,2

In general, heat and mass transfer coefficients were experimentally determined. For the ammonia sub-cooler and the solution heat exchanger, the experimental set supplied all the necessary data for that estimation; for all other exchangers, experimental data were the basis for a theoretical estimation of their coefficients.

Computation of the available evaporative NTU of the evaporative cooled exchangers, as expressed in Eqs. (66), (78) and (87), required the estimation of the mass transfer coefficient K_m , which was done according to Mizushina *et al.* (1967), assuming that water and air flow rates through each exchanger are proportional to its plane front surface. The estimate by Mizushina *et al.* (1967) of the external water film convective coefficient was also employed. The internal convective heat transfer coefficient was calculated according to the kind of exchanger: for the evaporative condenser, the equation presented by Shah (1979) was used in combination with the Dittus-Boelter relation (Incropera, 1990) for the film convective heat transfer coefficient; for the weak solution cooler and the absorber, the Dittus-Boelter relation was used in the turbulent case and the Sieder and Tate (Incropera, 1990) equation for laminar flow inside the tubes.

Table 2 shows the heat transfer surface and the estimated values of the global heat transfer coefficient for each exchanger, as well as the estimated mass transfer coefficients for the evaporative cooled exchangers used in the numerical simulation of the system.

Table 2. Heat transfer surface, heat and mass transfer coefficients.

Unit	A[m^2]	U [kW/m^2K]	K_m [kg/m^2s]
Condenser	10	0.78	0.19
Absorber	8.75	0.39	0.19
Weak solution cooler	2.5	0.52	0.19
Evaporator	6	0.27	
Ammonia sub-cooler	2.6	0.082	
Solutions heat exchanger	7	0.63	
Desorber	7.3	0.37	
Reflux condenser	2.4	0.26	

The Substitution-Newton-Raphson Method

According to the above model, the system to be solved is formed by the equations (1) to (88), along with the thermodynamic state relations and the equations for the pressure drops and the heat transfer coefficients. The solution algorithm is based on the Substitution-Newton-Raphson approach, explained in detail by Figueiredo *et al.* (2002), and briefly resumed here.

Lets us consider the sparse non-linear system **f(x)=0**, with N equations and N variables. Because it is sparse, many equations can be employed to express some of the variables as explicit functions of other variables. A careful inspection of the system may indicate that n variables, renamed **y**, and called effective variables, can be strategically chosen so that the remaining N-n variables, called substitution variables, can be explicitly found by using N-n equations from the set. In other words, the whole set of physically relevant variables **x** can be determined by the narrower set of effective variables **y** as an explicit function **x(y)**. This constitutes the Substitution part of the Substitution-Newton-Raphson method. If a set of guessed values is assigned to **y**, the complete set of variables **x** is determined by N-n equations that would be satisfied without residuals, within the range of arithmetic precision of the machine. Applying **x** to the remaining n equations produces residuals that are forced to vanish through the Newton-Raphson procedure by manipulating the effective variables **y**.

In the present problem, only ten effective variables were required, namely { $\dot{m}_2$, T_5 , T_7 , T_{16} , T_{19} , X_{10}, Y_2 , X_{18} , P_3 , P_7}. The remaining variables of the set are explicitly calculated as functions of the effective variables through the equations above except equations (64), (48), (76), (22), (05), (32), (53), (85), (16) and (17). The latter are the residual equations, which must be satisfied by means of the Newton-Raphson method. In other words, their residuals, represented below by a simplified form of the logarithmic mean temperature differences (LMTD), must be forced to vanish by manipulation of the effective variables through the Newton-Raphson code.

$$R[1] = NTU_C^A - NTU_C^R \quad (91)$$

$$R[2] = Q_E \ (UA)_E \ LMTD_E \quad (92)$$

$$R[3] = NTU_A^A - NTU_A^R \quad (93)$$

$$R[4] = Q_{RC} \ (UA)_{RC} \ LMTD_{RC} \quad (94)$$

$$R[5] = Q_D \ (UA)_D \ LMTD_D \quad (95)$$

$$R[6] = Q_{ASC} \ (UA)_{ASC} \ \Delta T_{ASC} \quad (96)$$

$$R[7] = Q_{SHx} \ (UA)_{SHx} \ LMTD_{SHx} \quad (97)$$

$$R[8] = NTU_{WSC}^A - NTU_{WSC}^R \quad (98)$$

$$R[9] = \dot{m}_r X_r + \dot{m}_1 Y_1 + \dot{m}_{16}(1-U_{16})X_{16} - \dot{m}_{17}X_{17} - \dot{m}_{1a}Y_{1a} \quad (99)$$

$$R[10] = \dot{m}_r h_r + \dot{m}_1 h_1 + \dot{m}_{16}(1-U_{16})h_{16}^L - \dot{m}_{17}h_{17} - \dot{m}_{1a}h_{1a} \quad (100)$$

Results

Results from the steady-state simulation of the system operation for an environment wet bulb temperature of 23ºC (the most representative in the region) are presented in Table 3, showing the internal thermodynamic parameters of the system. In this case, the COP was computed as 0,45.

Table 3. Simulated values and parameters.

Point	Estate	m [kg/s]	P [bar]	T[C]	X	Y	Z	H[kJ/kg] [kJ/kg]
1	V	0,031	13,01	118,10		0,8779	0,8779	1671,99
1b	L	0,008	12,92	101,17	0,3461		0,3461	249,16
1a	V	0,029	12,92	99,54		0,9448	0,9448	1542,08
R	L	0,008	12,73	40,00	0,7751		0,7751	25,98
2	V	0,023	12,73	40,00		0,9994	0,9994	1317,33
3	L	0,023	11,71	30,13	0,9994		0,9994	142,00
4	L	0,023	11,71	30,13	0,9994		0,9994	142,00
5	L	0,023	10,97	10,96	0,9994		0,9994	50,73
6	M	0,023	2,45	-14,06	0,9990	0,9999	0,9994	50,73
7	V	0,023	2,45	-11,46		0,9999	0,9999	1260,29
8	V	0,023	2,16	29,08		0,9994	0,9994	1351,56
9	M	0,174	1,65	45,23	0,2927	0,9635	0,3469	119,35
10	L	0,174	1,45	31,71	0,3469		0,3469	-83,05
11	L	0,174	1,45	31,71	0,3469		0,3469	-83,05
12	L	0,174	13,91	31,87	0,3469		0,3469	-81,32
13	L	0,174	13,51	31,87	0,3469		0,3469	-81,32
14	L	0,174	13,12	51,47	0,3469		0,3469	12,79
15	L	0,174	13,12	51,47	0,3469		0,3469	12,79
16	M	0,174	12,73	102,73	0,3409	0,9368	0,3469	269,57
17	L	0,182	13,01	101,17	0,3461		0,3461	249,16
18	L	0,151	13,01	118,10	0,2671		0,2671	361,64
19	L	0,151	11,71	57,10	0,2671		0,2671	73,45
20	L	0,151	11,31	35,30	0,2671		0,2671	-31,38
21	L	0,151	1,65	35,49	0,2671		0,2671	-31,38

Table 4 shows a comparison between experimental and simulated energy transfer rates and COP. Except for the pump, the maximum error is under 10%, an indication of the reliability of the mathematical model. Although errors due to the assumptions on the rectification efficiency and on the suction pressure can not be excluded, the differences between experiment and simulation are attributed mainly to experimental uncertainties, particularly with respect to the concentration, which was measured indirectly via density and temperature. Pump performance, in particular, was affected by a short period of cavitation and diminished pump volumetric efficiency after the defrost period, because the high-concentration solution temporally formed in the absorber is not sufficiently cooled – a consequence of the small absorber heat transfer area. This cavitation was not taken into consideration in the model, accounting for the difference between simulated and experimental pump work values.

Table 4. Comparison between simulated and experimental data.

Parameter	Experimental	Simulated	Relative error [%]
Q_E[kW]	21,43	22,66	5,74
Q_C[kW]	23,90	22,02	7,86
Q_A[kW]	35,57	34,79	2,79
Q_D[kW]	51,42	49,58	3,55
Q_R[kW]	15,75	16,18	2,66
Q_{AC}[kW]	1,67	1,71	2,39
Q_{WSC}[kW]	17,71	16,06	9,10
Q_{SSE}[kW]	40,22	44,14	9,75
W_P[kW]	0,57	0,48	15,7
COP[%]	41,94	45,32	9,87

Figure 2 gives a broad view of the external heat transfer rates of the system, namely those of the condenser, the evaporator, the absorber and the desorber, when the ambient wet-bulb temperature varies from 20ºC to 30ºC. Figure 3 shows the corresponding internal heat transfer rates for the ammonia cooler, the solution heat exchanger and the reflux condenser. All the external heat transfer rates diminishes with the increased wet-bulb temperature, in contrast with the internal heat transfer rates, which are unaffected by the external wet-bulb temperature.

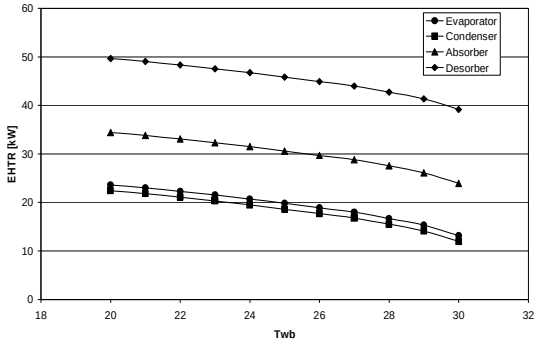

Figure 2. External heat transfer rates.

Although it is an external heat exchanger (exchanging heat directly with the surrounding air), the weak solution cooler was included in Fig. 3 to point out how close its heat transfer rate is to that of the reflux condenser, which shows that there is not heat recovery from the rectification process.

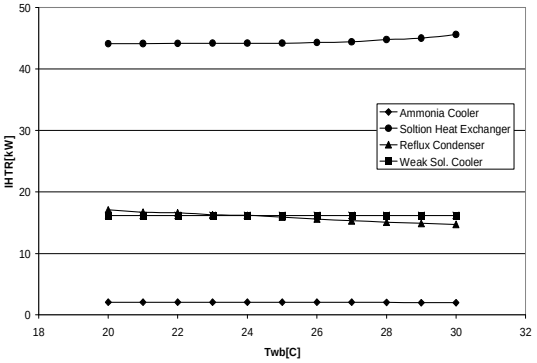

Figure 3. Internal heat transfer rates.

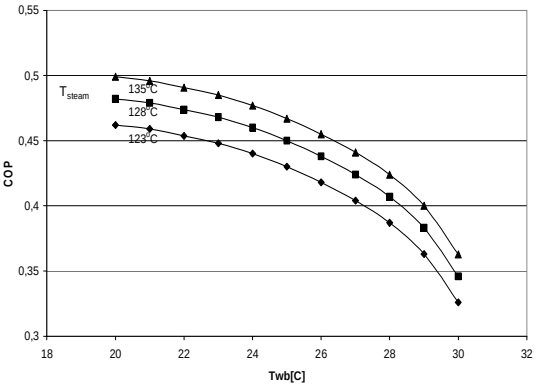

Figure 4. COP variation with steam and wet bulb temperatures.

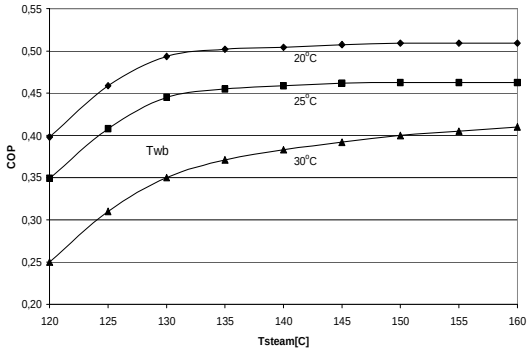

Figure 5. COP variation with steam and wet bulb temperatures.

Figures 4 and 5 show the variation of the COP with respect to the most relevant external parameters: ambient wet-bulb temperature and heating vapor temperature. Those figures indicate that, for the present evaporative cooled absorption system, the coefficient of performance has a greater dependence on ambient wet-bulb temperature than on steam temperature.

An examination of the actual temperatures of the cycle revealed that the absorption temperature is high, and leads to a poor performance of the absorption process. This suggests that the system performance could be considerably enhanced by increasing the heat and mass transfer surface of the absorber. This hypothesis is investigated with help of the mathematical model for steady-state operation by a comparison of different design optimization paths by varying the UA values of the main heat exchangers. The result can be seen in Figure 7, which shows the variation of the machine COP with respect to the UA values of different exchangers, keeping the remaining UA values unchanged in each case. The system COP is significantly worsened with the decrease of UA values below the design point, whereas improvement is small when UA values increase above the design point, except for the absorber UA value, for which an increase of 20% leads to a considerable improvement of about 10% in system COP, and an increase of 40% leads to a 15% rise in system COP.

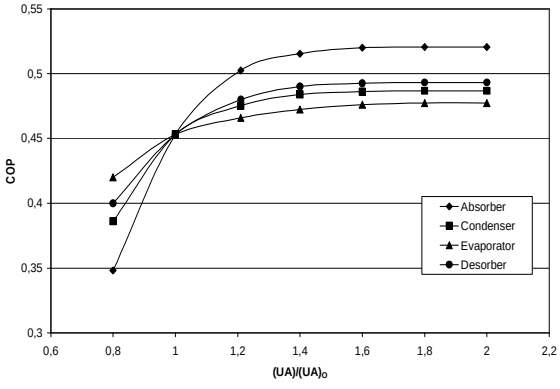

Figure 7. Variation of system COP with the relative UA values.

Conclusion

The mean conditions of operation of an evaporative cooled water-ammonia absorption system used for scale ice production was simulated by a steady-state model, and the main thermal parameters were compared with the respective values obtained from experimental mean values, showing good agreement.

The Successive-Newton-Raphson approach was successfully applied to the solution of a nonlinear system with more than 100 equations that constitute the mathematical model, drastically reducing the dimension of the equations system to 10 equations, which were then easily solved by the Newton-Raphson algorithm. Another important advantage of this approach, particularly in systems with a pronounced nonlinear behavior such as the water-ammonia system, is the reduced number of variables to be estimated initially, thus improving the conditions of convergence process.

The mathematical model has revealed that the efficiency of the absorption system could be improved by increasing the absorber heat transfer area. An increase of about 40% in the heat transfer surface of the absorber could improve the system COP by about 15%.

Acknowledgment

The authors would like to express their gratitude to the Foundation for the Support to Research of São Paulo State (FAPESP) by its partial support to this work.

References

Churchill, S. N. "Friction factor equation span all fluid flow regimes" *Chem. Eng.*, Nov. 1977, pp.91-92

Figueiredo, J. R.; Santos, R. G.; Favaro, C.; Silva, A. F. S. & Sbravati, A. "Substitution-Newton-Raphson Method applied to the Modeling of a Vapour Compression Refrigeration System Using Different Representations of the Thermodynamic Properties of R-134a" *J. of the Braz. Soc. Mechanical Sciences*, v.XXIV, pp.158-168 (2002).

Incropera, F. P. and De Witt, D. P. *Fundamentals of Heat and Mas Transfer*. John Wiley & Sons. 1990.

Kern, Q. D. *Process Heat Transfer*. MacGraw-Hill-Kogakusha, pp 313-373, 1950.

Leindenfrost, W. and Korenic, B. "Evaporative cooling and Heat Transfer augmentation Related to Reduced Condenser Temperatures". *Heat Transfer Eng*. Vol 3. No. 3-4. pp 38-56. 1982.

McLinden, M. O. and Klein, S.A. "Steady State modeling of Absorption Heat Pump with a Comparison to Experiments". *ASHRAE Transactions*, 91, Part 2b, 1793-1807. 1985.

Mizushina, T., Ito, R. and Miyashita, H. "Experimental Study of an Evaporative Cooler". *Int. Chem. Eng*. Vol. 7. No. 4, pp. 727-732. 1967.

Molt, K. "Termodynamische Modellierung von Prozesen ein und zwei stufiger Sorptionswãmerpumpe". *VDI Fortschrittdericht, Reihe* 6, Nr. 157, 1984.

Grossman, G. and Michelson, E. A modular computer simulation of absorption systems. *ASHRAE Transactions*. 91 (2b). 1808-1827. 1985.

Grossman, G. *et al*. "A computer model for simulation of absorption systems in flexible and modular form". *ASHRAE Transactions*. 93 (2). 2389-2428. 1987.

Grossman, G. *et al*. "A computer model for simulation of absorption systems in flexible and modular form". *ASHRAE Transactions*. 93 (2). 2389-2428. 1990.

Schultz, S. C. G. "Equations of state for the system ammonia-water for use with computer." *Proc. XIII Congress of Refrigeration*. Washington, 143. 1971.

Shah, M. M. "A general correlation for heat transfer during film condensation inside pipes", *Int. J.*

Heat Mass Transfer, 22, 547–556. 1979.

Silverio, R. J. R. "Análise e simulação de um sistema de absorção água-amônia para produção de gelo em escamas". In Portuguese. Dr. thesis. Mechanical Engineering School, UNICAMP. Campinas. SP. Brazil. 1999.

Vliet, G.C., Lawson, M.B. and Lithgow, R. A. "Water-Lithium Bromide Double effect Absorption cooling Cycle Analysis". *ASHRAE Transactions*, 88, part 1, 811 -823. 1982.

Webb, R. L. "A Unified Theoretical Treatment for Thermal Analysis of Cooling Towers, Evaporative Condensers, and Fluid Coolers". *ASHRAE Transactions*., V-90, Part 1. 1984.

Zigler, B. and Trepp, Ch. "Equation of State for ammonia-water mixtures". *Int. Journal of Refrigeration*. 7 (2). 101-106. 1984.